Time-resolved second-order coherence of an integrated biphoton frequency comb

Karthik V. Myilswamy,[1,†] Suparna Seshadri,[1,†], Junqiu Liu,[2] Tobias J. Kippenberg,[2] Andrew M. Weiner,[1] and Joseph M. Lukens[3,*]

[1]*School of Electrical and Computer Engineering and Purdue Quantum Science and Engineering Institute, Purdue University, West Lafayette, Indiana 47907, USA*
[2]*Institute of Physics, Swiss Federal Institute of Technology Lausanne (EPFL), CH-1015 Lausanne, Switzerland*
[3]*Quantum Information Science Section, Oak Ridge National Laboratory, Oak Ridge, Tennessee 37831, USA*

[†]*Equal contribution; *lukensjm@ornl.gov*

Abstract: We perform time-resolved second-order coherence characterization of multiple photon resonances from an integrated 40.5 GHz silicon nitride microring, using electro-optic modulation to observe interference effects otherwise hidden by detector jitter.

Integrated photonics plays an important role in the miniaturization and scalability of circuits for photonic quantum information processing. The frequency degree of freedom is particularly attractive as it allows for the generation of biphoton frequency combs (BFCs) containing a large number of frequency bins in a compact manner [1,2], making the statistical properties of such spectral modes of key significance to quantum information. For example, Hanbury Brown–Twiss (HBT) interferometry is a widely employed tool to measure the second-order correlation function $g^{(2)}(\tau)$ of unheralded signal or idler fields. Yet detector jitter frequently limits the precision of such measurements. While slow detectors that integrate over entire pulses still provide useful information—such as the number of Schmidt modes present in an entangled photon source [3]—the more general case of full time-resolved measurement remains of interest. For integrated BFCs specifically, *individual* comb lines often possess sufficiently narrow bandwidth for direct $g^{(2)}(\tau)$ measurement [4, 5], but typical free spectral ranges (FSRs) on the order of tens of GHz and beyond have prevented full resolution of $g^{(2)}(\tau)$ for *multiple* comb lines together. In this work, we generate a BFC from a silicon nitride (Si_3N_4) microring with an FSR of 40.5 GHz and externally phase modulate with a slightly detuned RF frequency, allowing us to directly resolve the fine features in $g^{(2)}(\tau)$ of the marginal signal field using commercial superconducting nanowire detectors (SNSPDs). We here note that we have utilized a similar scheme for probing the phase coherence of BFCs in our previous work [6].

Figure 1(a) illustrates the experimental setup. The Si_3N_4 microring used in our experiment was fabricated using the photonic Damascene reflow process [7]. Time-energy–entangled BFCs are generated via spontaneous four-wave mixing (SFWM). An amplified continuous-wave (CW) laser operating at one of the ring resonances (∼1550.9 nm) is used to pump the microring at a bus waveguide power of ∼14 mW, well below the parametric threshold (80 mW). The microring is overcoupled and features loaded and intrinsic Q-factors of $\sim 10^6$ and $\sim 10^7$, respectively. The measured linear through-port spectrum of the microring is shown in Fig. 1(c). Dense wavelength-division multiplexing filters are used before the ring to block the amplified spontaneous emission and after it to suppress the residual pump. We then use a programmable pulse shaper to select specific signal bins, followed by an electro-optic phase modulator (EOM) for sideband generation. We use another pulse shaper as a wavelength selective switch (WSS) to route the signal bins of interest to a 50:50 beamsplitter to perform HBT interferometry. The two arms on the output side of the beamsplitter are connected to SNSPDs followed by a time tagger to measure $g^{(2)}(\tau)$. As the idler photons are discarded and not used to herald we expect to observe thermal statistics [i.e., $g^{(2)}(0) = 2$]. For an SFWM process seeded by the CW pump, the second-order correlation function of the unheralded signal or idler field consisting of d identical frequency bins with Lorentzian lineshape of width γ and a bin separation of $\Delta\omega$ is given by [8]

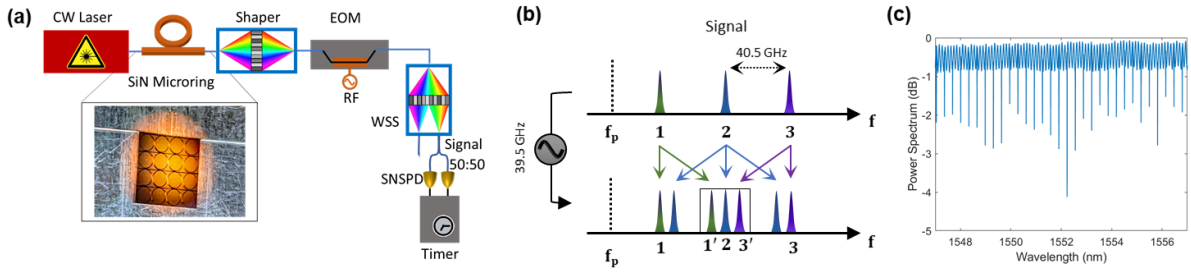

Fig. 1. (a) Experimental setup. (b) Illustration of phase modulated BFC (c) Linear through-port spectrum of microring.

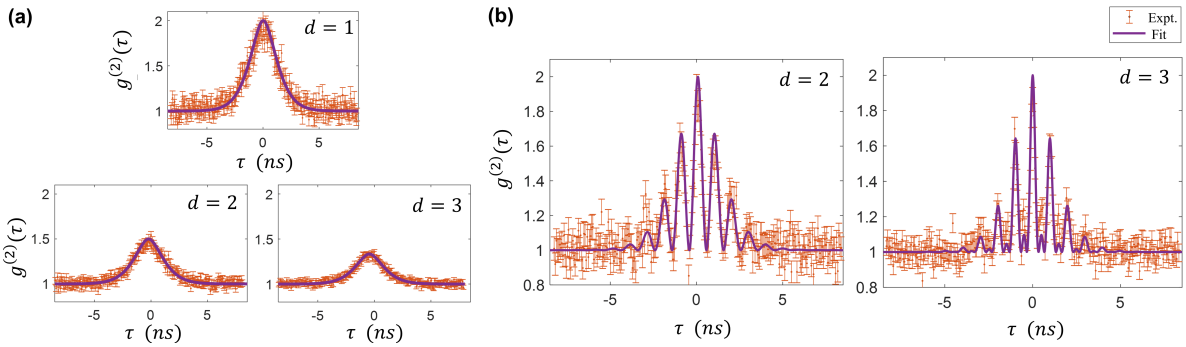

Fig. 2. Time-resolved second-order correlation measurements of the signal field with d bins. (a) Without RF modulation. (b) With RF modulation and spectral filtering. The coincidence histograms used to compute $g^{(2)}(\tau)$ in (a) and (b) are acquired over 15 mins and 120 mins, respectively. The histogram bin width is set to 64 ps.

$$g^{(2)}(\tau) = 1 + e^{-\gamma|\tau|}\left(1 + \frac{\gamma|\tau|}{2}\right)^2 \left|\frac{1}{d}\sum_{k=1}^{d} e^{ik\Delta\omega\tau}\right|^2, \tag{1}$$

where τ represents the delay between the arrival time of the two photons, γ decides the width of the exponentially decaying envelope, and $\Delta\omega$ dictates the multimode interference pattern within the envelope.

In our experiments, we worked with up to $d = 3$ signal bins (corresponding to resonances located 12, 13, and 14 FSRs away from the pump). In the first set of experiments, we do not apply RF modulation and directly send the d signal bins into the HBT interferometer. The $\sim$110 ps combined jitter of the SNSPDs averages out the interference fringes occurring in the timescale of $\sim$25 ps ($2\pi/\Delta\omega$). Such averaging in Eq. (1) results in a reduced peak value of $g^{(2)}(0) \approx 1 + \frac{1}{d}$. These results are shown in Fig. 2(a), where one can clearly see that any multimode interference features have been averaged out.

In order to resolve the fast features in $g^{(2)}(\tau)$, we now implement electro-optic modulation to generate frequency sidebands such that the sidebands from different bins fall close to each other with a small detuning. Selecting an RF frequency of 39.5 GHz—1 GHz smaller than the FSR—we effectively generate a new set of BFC lines with $\Delta\omega/2\pi = 1$ GHz, enabling time-resolved measurement of $g^{(2)}(\tau)$ with the fine features intact. Our proposed scheme for up to $d = 3$ is shown in Fig. 1(b). We only pass the signal photons around the central frequency bin into the HBT interferometer, which contain sideband contributions from the adjacent frequency bins. The results corresponding to $d = 2$ and $d = 3$ are plotted in Fig. 2(b). The experimental results are in excellent agreement with the theoretical fits, demonstrating the multimode interference patterns within the envelope. From the theoretical fits, we find $\gamma/2\pi \approx 200$ MHz (consistent with linear spectroscopy) and $\Delta\omega/2\pi = 1$ GHz, as expected. Importantly, with the improved effective resolution, we obtain $g^{(2)}(0) = 2$ directly, confirming the presence of thermal statistics for superpositions of multiple bins—a feature previously hidden in the washed-out results of Fig. 2(a).

This research was performed in part at Oak Ridge National Laboratory, managed by UT-Battelle, LLC, for the U.S. Department of Energy under contract no. DE-AC05-00OR22725. Funding was provided by the U.S. Department of Energy (Early Career Research Program); the National Science Foundation (1839191-ECCS, 2034019-ECCS, DMR-1747426); the Air Force Office of Scientific Research (Award no. FA9550-19-1-0250); and the Swiss National Science Foundation (Grant no. 176563).

References

1. M. Kues, C. Reimer, P. Roztocki, L. R. Cortés, S. Sciara, B. Wetzel, Y. Zhang, A. Cino, S. T. Chu, B. E. Little, D. J. Moss, L. Caspani, J. Azaña, and R. Morandotti, Nature **546**, 622 (2017).
2. P. Imany, J. A. Jaramillo-Villegas, O. D. Odele, K. Han, D. E. Leaird, J. M. Lukens, P. Lougovski, M. Qi, and A. M. Weiner, Opt. Express **26**, 1825 (2018).
3. A. Christ, K. Laiho, A. Eckstein, K. N. Cassemiro, and C. Silberhorn, New J. Phys. **13**, 033027 (2011).
4. X. Guo, C. L.Zou, C. Schuck, H. Jung, R. Cheng, and H. X.Tang, Light Sci. Appl. **6**, e16249 (2017).
5. F. Samara, N. Maring, A. Martin, A. Raja, T. Kippenberg, H. Zbinden, and R. Thew, Quantum Sci. Technol. **6**, 045024 (2021).
6. K. V. Myilswamy, M. S. Alshaykh, H.-H. Lu, J. Liu, D. E. Leaird, T. J. Kippenberg, and A. M. Weiner, CLEO, paper JM3F.5 (2021).
7. J. Liu, G. Huang, R. N. Wang, J. He, A. S. Raja, T. Liu, N. J. Engelsen, and T. J. Kippenberg, Nat. Commun. **12**, 2236 (2021).
8. K. H. Luo, H. Herrmann, S. Krapick, B. Brecht, R. Ricken, V. Quiring, H. Suche, W. Sohler, and C. Silberhorn, New J. Phys. **17**, 073039 (2015).